Journal of The Electrochemical Society, **159** (1) B86-B89 (2012)
0013-4651/2012/159(1)/B86/4/$28.00 © The Electrochemical Society

Highly Durable Graphene Nanosheet Supported Iron Catalyst for Oxygen Reduction Reaction in PEM Fuel Cells

Ja-Yeon Choi, Drew Higgins,* and Zhongwei Chen,z**

Department of Chemical Engineering, Waterloo Institute for Nanotechnology, Waterloo Institute for Sustainable Energy, University of Waterloo, Waterloo, Ontario, Canada N2L 3G1

A novel NPMC using pyrimidine-2,4,5,6-tetramine sulfuric acid hydrate (PTAm) as a nitrogen precursor and graphene nanosheets as catalyst supports was prepared and characterized. We investigate the effect of different pyrolysis temperatures on the catalysts' ORR activity along with detailed surface analysis to provide insight regarding the nature of the ORR active surface moieties. The NPMC sample heat treated at 800°C was found to display optimal ORR activity and H_2O selectivity, specifically, an onset potential of 0.853 V vs RHE, a half-wave potential of 0.682 V vs RHE, and a H_2O selectivity of ca. 99.9%. High stability through an accelerated durability testing (ADT) protocol was demonstrated and attributed to the high graphitic content of the catalyst support material. This novel NPMC demonstrates promising electrocatalyst activity and superior durability over commercial Pt/C catalyst for ORR under the studied conditions, rendering graphene nanosheets as an ideal replacement to traditional nanostructured carbon support materials.
 [DOI: 10.1149/2.062201jes]

Manuscript submitted August 23, 2011; revised manuscript received October 12, 2011. Published December 14, 2011.

While platinum is the most commonly used catalyst material for the oxygen reduction reaction (ORR) occurring at the cathode of polymer electrolyte membrane fuel cells (PEMFCs), the high cost and limited natural abundance of this noble metal still limits the large-scale commercialization of this technology.[1,2] As a substitute for platinum, the development of non-precious metal catalysts (NPMCs) with high ORR activity and practical durability has been viewed as the long-term solution to reduce the overall cost of PEMFC systems.[3–5] Despite ample investigations being done with steady progress realized in this field, the performance of even the best NPMCs is still inferior to that of precious metal catalysts and thus it is a stringent necessity to develop alternative preparation strategies to improve the ORR activity and the durability of NPMCs.[6–8] Utilization of carbon support materials with unique structural and physical properties has been demonstrated as a feasible method to tailor the catalytic activity and the stability of NPMC composites,[9] owing to the specific catalyst-support interactions and favorable carbon support properties including porosity, high surface areas, electronic conductivity and electrochemical stability. Specifically, significant efforts have been devoted to the utilization of novel nanostructured carbon supports with large surface areas and pore volumes, including carbon nanotubes,[10] carbon nanofibers,[11] and mesoporous carbons.[12] Despite promising performance achieved in terms of ORR activity using these nanostructured support materials, there is still enormous demand and potential for NPMC improvement, especially in durability.

Graphene, consisting of a two-dimensional (2D) monolayer of graphitic carbon atoms, has been viewed as a promising candidate for the fuel cell catalyst support, due to its many intriguing properties such as high aspect ratios, large surface areas, rich electronic states, good electron transport, thermal/chemical stability and good mechanical properties.[13,14] Scientists have already developed graphene based metal-free fuel cell catalysts showing better ORR activity and durability than the commercial Pt/C catalyst in alkaline condition,[14–16] however, despite the immense promise of these materials, the application of graphene as a NPMC support remains essentially unexplored, especially in acidic electrolyte conditions. In the present study, we report the development of a novel NPMC in acid electrolyte using pyrimidine-2,4,5,6-tetramine sulfuric acid hydrate (PTAm) as a nitrogen precursor and graphene nanosheets as catalyst supports. We investigate the effect of different pyrolysis temperatures on the catalysts' ORR activity along with detailed surface analysis to provide insight regarding the nature of the ORR active surface moieties. This novel NPMC demonstrates promising electrocatalyst activity and durability superior to that of commercial catalyst for the ORR, rendering graphene nanosheets as a suitable replacement to traditional nanostructured carbon support materials.

* Electrochemical Society Student Member.
** Electrochemical Society Active Member.
z E-mail: zhwchen@uwaterloo.ca

Experimental

To prepare graphene nanosheet supported NPMCs using PTAm as a nitrogen precursor and iron acetate (FeAc) as a metal precursor, a desired amount of graphene and PTAm was added to 4M HCl solution, and the solution was subjected to low temperature heat treatment at 80°C for 24 h while stirring. The proposed coupling reaction between the support and PTAm is illustrated in Figure 1a.[17] The mixture was filtered, washed with deionized water and dried overnight in an oven at 60°C. The dried sample was then ground to a fine powder and ultrasonically mixed with 1 wt.% FeAc in 50 mL of ethanol for one hour. The solution was again filtered and dried in an oven. The remaining dried precipitate was pyrolyzed at various temperatures ranging from 700 to 1000°C for one hour under nitrogen gas flow. These catalysts are referred as FPGNP (non-pyrolyzed), FPG700, FPG800, FPG900 and FPG1000 accordingly.

The electrocatalytic activity was evaluated in a three-electrode electrochemical cell using a Pine-Instrument's Bipotentiostat AFCBP1, equipped with a speed rotator. All RDE measurements were performed in acidic 0.1 M $HClO_4$ electrolyte at room temperature, using a Ag/AgCl reference electrode. To prepare the glassy carbon working electrode (0.19635 cm^2), 4 mg of catalyst sample was ultrasonically dispersed in 1 mL of ethanol. 30 μL of the ink and 5 μL of 0.5 wt.% Nafion solution were applied to the glassy carbon disk, leading to identical electrode catalyst loadings for each sample during testing. ORR curves were recorded at a scan rate of 10 mV/s with the electrolyte saturated with oxygen gas under various electrode rotation speeds (100, 400, 900 and 1600 rpm). ORR curves were corrected by removing background currents obtained under the same testing conditions in nitrogen saturated electrolyte. Transmission electron microscopy (TEM) was utilized to observe the surface morphology, and X-ray photoelectron spectroscopy (XPS) was conducted to determine surface atomic compositions and configurations.

Results and Discussion

The morphology of FPG800 observed by TEM is displayed in Figure 1b. Many small graphene nanoplatelets were observed clustered together, possibly resulting from the linkage between PTAm molecules and adjacent graphene sheets, since PTAm contains many nitrogen sites that can be coupled to the edge plane of the graphene and the functional groups.[17] These adjacent graphene nanosheet

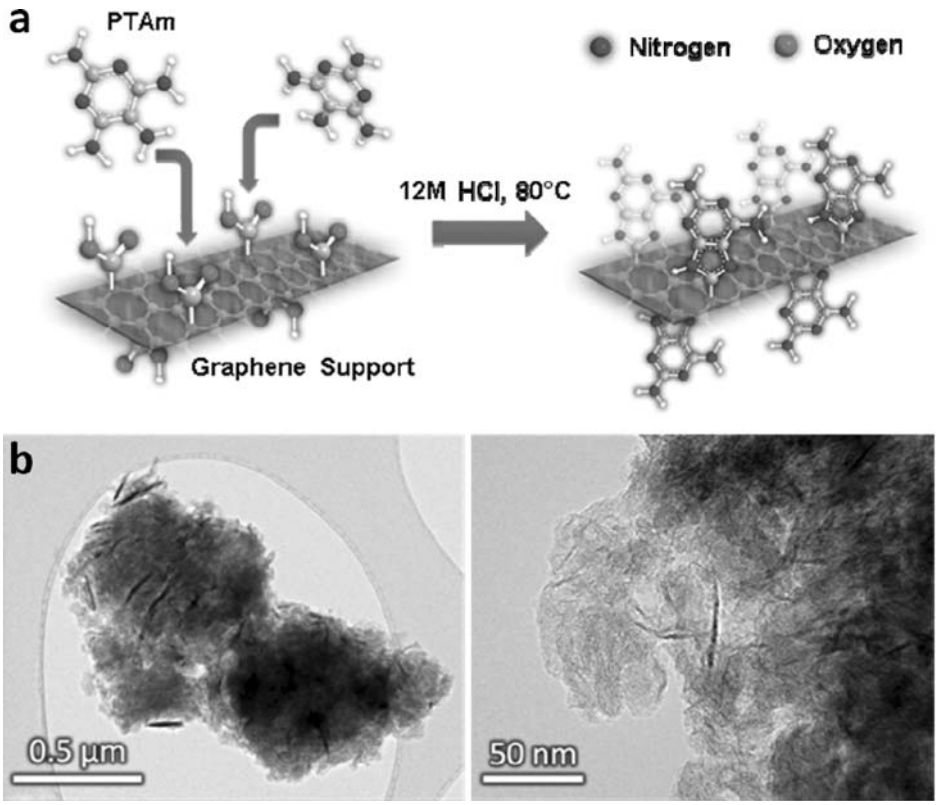

Figure 1. (a) Proposed schematic representation of the coupling reaction of pyrimidine-2,4,5,6-tetramine sulfuric acid hydrate to graphene nanosheets. (b) Two TEM images of Fe-PTAm/Graphene pyrolyzed at 800°C, obtained at different magnifications.

clusters can serve to host one of the most promising metal-nitrogen active sites structures upon pyrolysis.[18]

Half-cell RRDE experiments were conducted for all samples to determine their catalytic activity for the ORR, with polarization curves plotted in Figure 2a at a rotation rate of 900 rpm. From these results, it is clear that a pyrolysis step is crucial, where FPGNP demonstrated negligible ORR activity. FPG800 displayed optimal activity, demonstrating an onset potential of 0.853 V and a half-wave potential of 0.692 V (vs. RHE) and full RRDE data at various rotation rates provided in Figure 2b. At pyrolysis temperatures above or below 800°C reduced onset potentials and current densities were observed. Moreover, the H_2O selectivity of these samples was determined from ring current data, with high selectivity values providing indication of a more efficient 4 electron reduction pathway compared to the inefficient 2 electron reduction forming destructive H_2O_2 species. Figure 3 provides H_2O selectivity of all four pyrolyzed graphene based catalysts with the order of highest to lowest H_2O selectivities being FPG800 > FPG900 > FPG 1000 and FPG700, consistent with ORR activity results. Specifically, FPG800 shows the best H_2O selectivity of 99.9% at 0.4 V vs. RHE, indicating negligible selectivity towards the two electron reduction pathway. The results of the onset potentials, current densities obtained at 0.6V vs. RHE and H_2O selectivities are tabulated in Table I for all synthesized catalysts.

To evaluate the effect of utilizing graphene as the NPMC support, the same type of catalyst was fabricated using Ketjen 600JD carbon black support. This porous carbon has been previously established as a good electrocatalyst support and thus serves as a good performance evaluation benchmark. Catalyst synthesis conditions were identical with the NPMC, with the exception of the carbon support material utilized. Pyrolysis was carried out at the same temperatures as well; however, the activity of only the highest performing material pyrolyzed at 900°C is illustrated in Figure 3a. From the presented curves, it can clearly be seen that the ORR performance of the graphene based catalysts exceeds that of the ketjen black based catalyst for this type of catalyst, which effectively demonstrates the promising potential for the graphene as a catalyst support.

The durability of FPG800 was investigated by accelerated degradation testing (ADT) consisting of 1000 cycles in N2 saturated electrolyte at a scan rate of 50 mV/s between 0 and 1.2 V vs. RHE. Durability data is provided in Figure 4 along with commercial carbon supported platinum (Pt/C) for comparison. Surprisingly, FPG800 showed only a slight decrease of 0.055 V in the half-wave potential while Pt/C showed a much higher potential decrease of 0.125 V. Moreover, the current densities obtained at 0.2 V vs. RHE before and after the cycles for FPG800 showed almost no difference (0.016 mA/cm^2) while the difference for Pt/C was 0.055 mA/cm^2. The resulting current density at 0.2 V vs. RHE for FPG800 following ADT

Table I. Summary of RRDE experiments for synthesized catalyst samples.

	Current Density at 0.6 V vs. RHE (mA/cm^2)	Onset Potential (V vs. RHE)	H_2O Selectivity at 0.4 V vs. RHE (%)
FPGNP	0.01	0.446	
FPG700	2.88	0.839	99.3
FPG800	4.12	0.853	99.9
FPG900	3.75	0.845	99.6
FPG1000	3.32	0.836	99.5
FPK900	3.49	0.838	

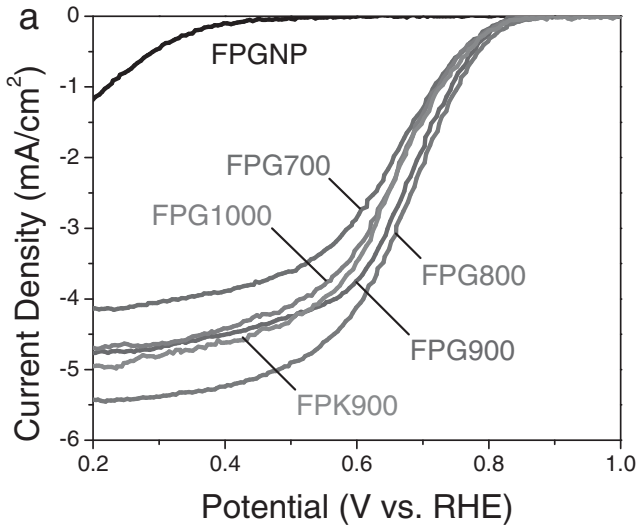

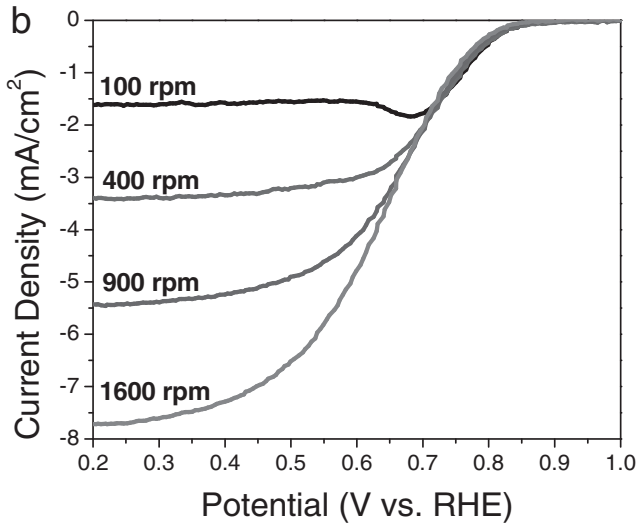

Figure 2. (a) ORR curves of Fe-PTAm/Graphene catalysts heat-treated in N_2 using different pyrolysis temperatures, obtained at 900 rpm. (b) ORR curves of FPG800 at various rotation speeds.

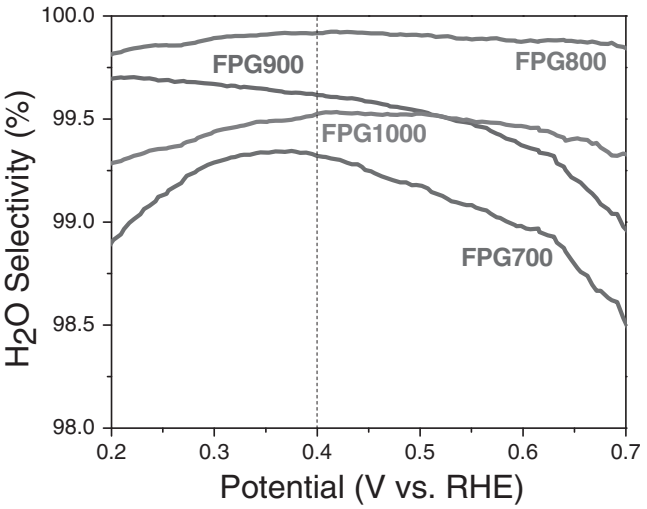

Figure 3. H_2O selectivity for the Fe-PTAm/Graphene catalysts, obtained at 900 rpm.

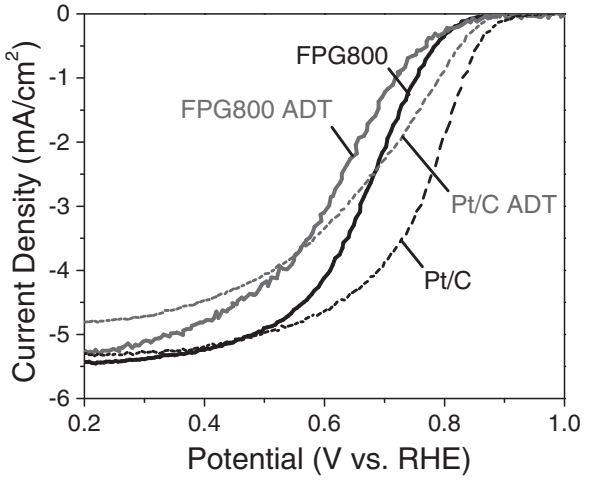

Figure 4. ORR curves of FPG800 before and after running 1000 CV cycles in nitrogen saturated electrolyte, obtained at 900 rpm.

was approximately 10% higher than that of the commercial catalyst. Overall, FPG800 showed superior durability than that of the commercial carbon supported platinum catalyst under the studied conditions. This provides indication of the promising stability of these materials most likely arising due to the high graphitic content.[15]

XPS was utilized to determine the surface atomic composition and chemistry of the catalyst samples. XPS confirmed the presence of a variety of carbon, and nitrogen species, along with trace amounts of iron as illustrated in Figure 5. A decreasing trend was observed for the surface nitrogen content with increasing pyrolysis temperatures, consistent with previous reports indicating decomposition of nitrogen species at elevated temperatures.[19] High resolution N1s spectra along with a detailed breakdown of the contributing species obtained after peak de-convolution are provided in Figure 6 and 7, respectively. It should be noted that the scale for the intensity obtained for each catalyst has been adjusted for better visibility in Fig. 6. Specifically, the N1s spectra was broken down into three peaks representing pyridinic (398.3 eV), pyrrolic (400.5 ~ 401 eV), and quaternary (401 ~ 403 eV) nitrogen functionalities.[20] Following pyrolysis at 700°C, the relative amount of pyridinic nitrogen increased to 59.41 at.% of all the nitrogen groups, and dropped slightly to 54.79 at.% for the sample pyrolyzed at 800°C. By further increasing the final pyrolysis temperature, the relative amount of pyridinic nitrogen decreases, as these species are relatively unstable at temperatures exceeding 800°C.[21] The slight decrease in the relative amount of pyridinic nitrogen from 700 to

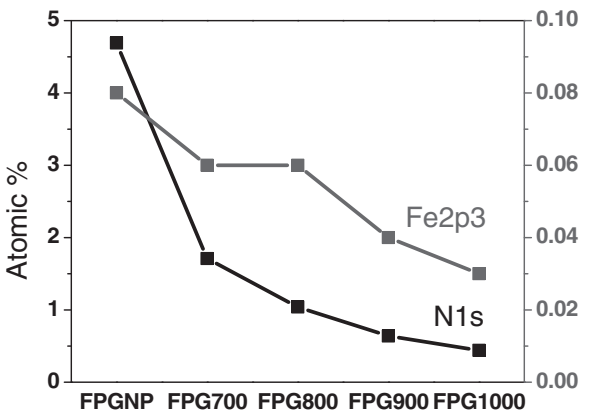

Figure 5. XPS summary of surface atomic composition of Fe-PTAm/Graphene catalysts.

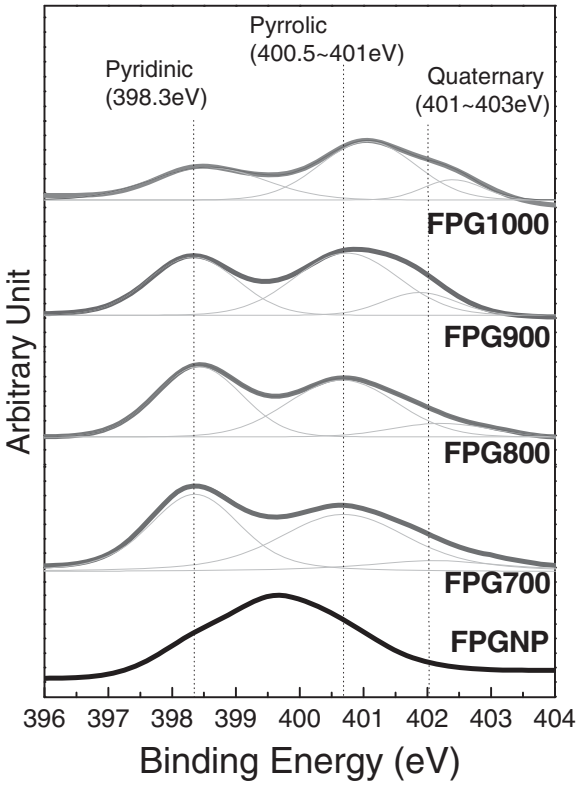

Figure 6. N 1s narrow scan spectra of the various FPG samples.

800°C, combined with a stable iron surface content observed from 700 to 800°C despite significant changes in the observed ORR activity can possibly indicate specific active site formation, or a transition of the active site from FeN_4/C to FeN_{2+2}/C structures. It has been reported that, while FeN_4/C is the most prominent active site at lower pyrolysis temperatures FeN_{2+2}/C catalytically active sites arise in the range of 700 to 800°C and reach the highest concentration at 800°C.[22] It has also been reported previously for catalysts using FeAc as the iron precursor and with low iron content (less than 0.2 wt%), FeN_{2+2}/C active sites dominate the catalytic behavior, while forming better electrical contact with the conductive graphene plane.[22,23] Moreover, as

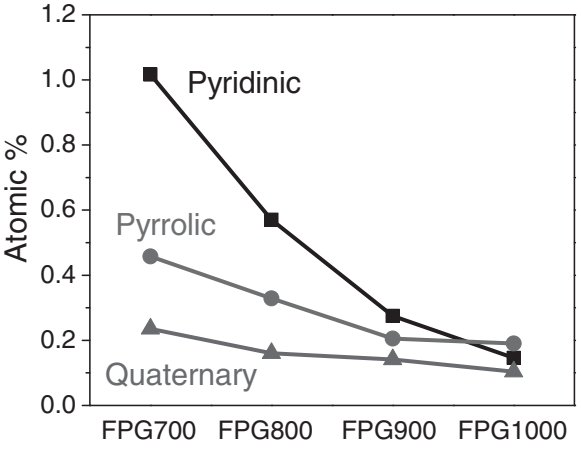

Figure 7. Nitrogen content of the various FPG samples.

it can be seen in Figure 7 the relative amount of pyrrolic and quaternary nitrogen increases with increased pyrolysis temperature, as these forms of nitrogen are stable at higher temperatures.[21] Thus, for this particular NPMC, there is no correlation between these two nitrogen groups and the performance. Thus, the catalyst performance reaches the highest at the temperature of 800°C and drops with increasing temperature due to both FeN_{2+2}/C active site and the overall nitrogen content decrease.

Conclusions

We have successfully synthesized a novel NPMC using PTAm as a nitrogen precursor, FeAc as iron precursor and graphene nanosheets as a catalyst support. This NPMC demonstrates promising electrocatalytic activity and durability for the ORR, rendering graphene nanosheets as a suitable replacement to traditional nanostructured carbon support materials. A pyrolysis procedure was deemed crucial for active site formation, where the NPMC sample heat treated at 800°C was found to display optimal ORR activity and H_2O selectivity, specifically, an onset potential of 0.853 V vs RHE, a half-wave potential of 0.682 V vs RHE, and a H_2O selectivity of ca. 99.9%. Moreover, high stability through ADT was demonstrated most likely due to the high graphitic content of the catalyst support material. Thus, graphene nanosheets are presented as an ideal catalyst support material, with promising ORR activity and stability demonstrated. Future investigations will focus on catalyst optimization by varying iron precursor loading and synthesis conditions, which have previously been deemed important factors influencing the ORR activity.

Acknowledgments

This work was financially supported by the Natural Sciences and Engineering Research Council of Canada (NSERC) and the University of Waterloo.

References

1. D. C. Higgins, D. Meza, and Z. W. Chen, *J. Phys. Chem. C*, **114**, 21982 (2010).
2. X. Li, S. Park, and B. N. Popov, *J. Power Sources*, **195**, 445 (2010).
3. T. E. Wood, Z. Tan, A. K. Schmoeckel, D. O'Neill, and R. Atanasoski, *J. Power Sources*, **178**, 510 (2008).
4. W. M. Li, A. P. Yu, D. C. Higgins, B. G. Llanos, and Z. W. Chen, *J. Am. Chem. Soc.*, **132**, 17056 (2010).
5. Z. W. Chen, D. C. Higgins, A. Yu, L. Zhang, and J. Zhang, *Energ. Environ. Sci.*, **4**, 3167 (2011).
6. X. Li, G. Liu, and B. N. Popov, *J. Power Sources*, **195**, 6373 (2010).
7. G. Wu, K. L. More, C. M. Johnston, and P. Zelenay, *Science*, **332**, 443 (2011).
8. R. Baker, D. P. Wilkinson, and J. Zhang, *Electrochim. Acta*, **53**, 6906 (2008).
9. F. Jaouen, E. Proietti, M. Lefevre, R. Chenitz, J.-P. Dodelet, G. Wu, H. T. Chung, C. M. Johnston, and P. Zelenay, *Energ. Environ. Sci.*, **4**, 114 (2011).
10. Z. Chen, D. Higgins, H. Tao, R. S. Hsu, and Z. Chen, *J. Phys. Chem. C*, **113**, 21008 (2009).
11. T. Palaniselvam, R. Kannan, and S. Kurungot, *Chem. Commun.*, **47**, 2910 (2011).
12. J. Y. Choi, R. S. Hsu, and Z. W. Chen, *J. Phys. Chem. C.*, **114**, 8048 (2010).
13. A. K. Geim and K. S. Novoselov, *Nat. Mater.*, **6**, 183 (2007).
14. S. Yang, X. Feng, X. Wang, and K. Müllen, *Angewandte Chemie*, **50**, 5339 (2011).
15. D. S. Geng, Y. Chen, Y. G. Chen, Y. L. Li, R. Y. Li, X. L. Sun, S. Y. Ye, and S. Knights, *Energ. Environ. Sci.*, **4**, 760 (2011).
16. Y. Q. Sun, C. Li, Y. X. Xu, H. Bai, Z. Y. Yao, and G. Q. Shi, *Chem. Commun.*, **46**, 4740 (2010).
17. R. D. L. Smith and P. G. Pickup, *Electrochem. Commun.*, **11**, 10 (2009).
18. M. Lefèvre, E. Proietti, F. Jaouen, and J.-P. Dodelet, *Science*, **324**, 71 (2009).
19. G. Wu, C. M. Johnston, N. H. Mack, K. Artyushkova, M. Ferrandon, M. Nelson, J. S. Lezama-Pacheco, S. D. Conradson, K. L. More, D. J. Myers, and P. Zelenay, *J. Mater. Chem.*, **21**, 11392 (2011).
20. F. Jaouen, J. Herranz, M. Lefèvre, J.-P. Dodelet, U. I. Kramm, I. Herrmann, P. Bogdanoff, J. Maruyama, T. Nagaoka, A. Garsuch, J. R. Dahn, T. Olson, S. Pylypenko, P. Atanassov, and E. a. Ustinov, *ACS appl. Mater. Int.*, **1**, 1623 (2009).
21. P. H. Matter, L. Zhang, and U. S. Ozkan, *J. Catal.*, **239**, 83 (2006).
22. M. Lefevre, J. P. Dodelet, and P. Bertrand, *J. Phys. Chem. B*, **106**, 8705 (2002).
23. F. Charreteur, F. Jaouen, S. Ruggeri, and J. P. Dodelet, *Electrochim. Acta*, **53**, 2925 (2008).